Spatio-Temporal Analysis and Isopath Dynamics of Citrus Scab in Nursery Plots

T. R. Gottwald

Research Plant Pathologist, U.S. Department of Agriculture, ARS, Horticultural Research Laboratory, Orlando, FL 32803.
I thank C. L. Campbell, G. Hughes, and D. Chellemi for critical review and suggestions and P. Bell, A. Dow, C. Ferriola, and J. Bittle for technical assistance.
Accepted for publication 10 July 1995.

ABSTRACT

Gottwald, T. R. 1995 Spatio-temporal analysis and isopath dynamics of citrus scab in nursery plots. Phytopathology 85:1082-1092.

The Gompertz model was selected over three other models to describe temporal progress of disease incidence of citrus scab, caused by *Elsinoe fawcettii*, in four nurseries and eight disease control test plots of sour orange in Florida. Aggregation of disease was indicated by spatial autocorrelation analysis for nursery plots for all but one assessment date in one nursery. In three of the four nurseries, isopath boundaries moved predominately northward and away from a central focus of disease, presumably in response to splash dispersal of inoculum resulting from both rain showers and sprinkler irrigation. For the four nurseries and the eight disease control test plots, the spatial rate of spread (v) generally was greater early in the epidemics and when measured at distances further from the focus of infection. Rates of scab increase were reduced significantly in disease control plots by applications of captafol or copper at 30-day intervals compared to a water spray control. For all 12 plots, three-dimensional response surfaces of isopath-bounded areas (A_i) versus isopath level (I_α) and time (t) in days were fit to complex models via nonlinear regression. The best spatio-temporal model (log-normal additive with synergy and intercept) accounted for >95% of the variation in the data for all 12 data sets. Comparison among observed and predicted spatio-temporal data sets demonstrated that captafol significantly affected the spatio-temporal dynamics of citrus scab epidemics by reducing both inoculum production and providing protection to susceptible new leaves, whereas other control strategies did not.

Additional keywords: host growth, fungicide, *Sphaceloma fawcettii*.

In Florida, two biotypes of the citrus scab organism, *Elsinoe fawcettii* Bitancourt & Jenk., are present and are distinguished by their host range of citrus and citrus relatives (5,6,10,33). Both biotypes commonly are found in association with rough lemon, *Citrus limon*; grapefruit, *C.* × *paradisi*; and 'Murcott,' *C. reticulata*. However, only the sour orange biotype is capable of infecting sour orange, *C. aurantium* L.; fruits of 'Temple' orange, *C. temple*; and sweet orange cultivars, *C. sinensis* (38). In Florida, only the anamorph of the scab fungus, *Sphaceloma fawcettii* Jenk., has been found (5,6,10,32,33). Both hyaline and pigmented conidia have been described (19,32).

Hyaline elliptical conidia are susceptible to desiccation and, thus, are often short-lived, whereas pigmented conidia are more resistant to desiccation and have greater potential for survival. Free moisture is required for conidia production. Hyaline conidia either germinate directly when wetted or bud to form additional hyaline conidia. Pigmented, spindle-shaped conidia do not appear to germinate but rather give rise to hyaline conidia when wetted (32, 35).

Dispersal of conidia is primarily by water splash, although both types of conidia also are disseminated by winds in excess of 2 m/s (32,35). Splash dispersal has been implicated as being more important than wind dispersal in disease increase; however, the extended survival and resistance to desiccation of pigmented conidia point to their potential epidemiological significance for long-distance, wind dispersal (32).

The enhancement of scab epidemic development by irrigation also has been observed (9,32). Conidia require free water for a minimum of 1.5 to 2.5 h for germination and infection (9,32,40). Citrus foliage is susceptible to scab for only a short time after emerging from the bud and becomes resistant when less than 25% expanded.

Citrus scab can cause severe deformation of foliage and stunting of certain citrus rootstocks, especially sour orange when grown in citrus nurseries. The result is poorer quality and smaller caliper of rootstocks for budding. Nursery scab control has been most successfully achieved by fungicide application (10,15,16,24,26, 31,34,36,39). The fungicides captafol (Difolatan), benomyl (Benlate), ferbam (Vancide Fe), and various copper-containing compounds have been utilized and are listed here in order of decreasing effectiveness (34,35,36,37,38). The most effective compound, captafol, is no longer registered for control of citrus scab. The presence of benomyl-tolerant strains of *E. fawcettii* in Florida groves and nurseries and the reduced effectiveness of benomyl in the presence of these strains have been demonstrated (36). Therefore, at present there is a heavy reliance on copper-containing compounds for scab control.

Several simple models have been used to describe temporal disease development in terms of disease incidence and severity (3, 17,20,24,25,27,31). The Modjeska and Rawlings spatial autocorrelation model has been used to evaluate aggregation of diseased plants within and across rows, as well as the relative strength of aggregation and directionality or orientation of aggregation of crops planted in a regular lattice (11,12,23). The movement or velocity of "waves" of disease of given severity levels (isopaths) has been used to describe the spatial change in disease over time (18,21,22,28,29). Isopathic rates (velocities) of disease have been utilized to compare spatial spread of disease among cultivars and different chemical treatments (2,4,21,22). It also has been shown that the slope (b) of disease incidence (transformed with the log-

Corresponding author: T. R. Gottwald; E-mail address: gott@magicnet.net

istic or Gompertz model) regressed on the distance (15), the apparent infection rate (r or k), and the velocity of spatial disease spread (v) is related by the expression $v = rs|b^{-1}|$, where s = distance in meters (7,14).

The objectives of this study were to examine the potential for spatial and temporal development of citrus scab in noncontrolled nursery situations and in disease control plots to examine the effect of various historical and contemporary control measures of differing efficacy on epidemic development to gain a greater understanding of the spatio-temporal dynamics of citrus scab and to ascertain some of the reasons that currently registered control measures are less effective than those used in the past.

MATERIALS AND METHODS

Nursery plot design. Two simulated citrus nurseries were established during May 1987 at the USDA, ARS, A. H. Whitmore Foundation Farm in Lake County, FL. Each nursery consisted of 1,007 disease-free, greenhouse-grown sour orange seedlings planted in 19 rows with 53 plants per row. Rows were 0.76 m apart, and plants were 0.3 m apart within the row. The first nursery (87S) was planted with disease-free plants and acted as an indicator of exogenous inoculum. The central plant in the second nursery (87N) was replaced with a single severely scabbed sour orange seedling taken from a seedbed heavily infected with sour orange scab to serve as a focus of infection. The closest citrus grove to the plots, and a possible source of external scab inoculum, was located approximately 100 m to the southwest. During 1990, two more citrus nursery blocks (90S and 90N) were established at the USDA, ARS, Plymouth research facility in Seminole County, FL. These plots consisted of 13 rows each with 31 sour orange seedlings per row and were planted using the same plant spacing used in 1987. The central tree in each plot was replaced with a heavily infected sour orange tree as described earlier.

Design of disease control test plots. To examine the efficacy of historical and current chemical control measures on temporal disease development, four plots were established during May 1988 and four more during 1990 at the locations described earlier. Each plot consisted of five rows of 50 disease-free, greenhouse-grown sour orange plants per row with the same row and plant spacing described earlier. Rows were oriented north-south, and a scab-infected plant was added to the southern end of each row. These additional plants were severely diseased, sour orange seedlings taken from a heavily infected seedbed. Thus, five scab-infected plants at the southern end of each plot served as a line source of inoculum for a 'race track' type of plot. Disease-source plants were assessed for disease prior to planting, and each plot was established with plants of equal size, vigor, and disease incidence.

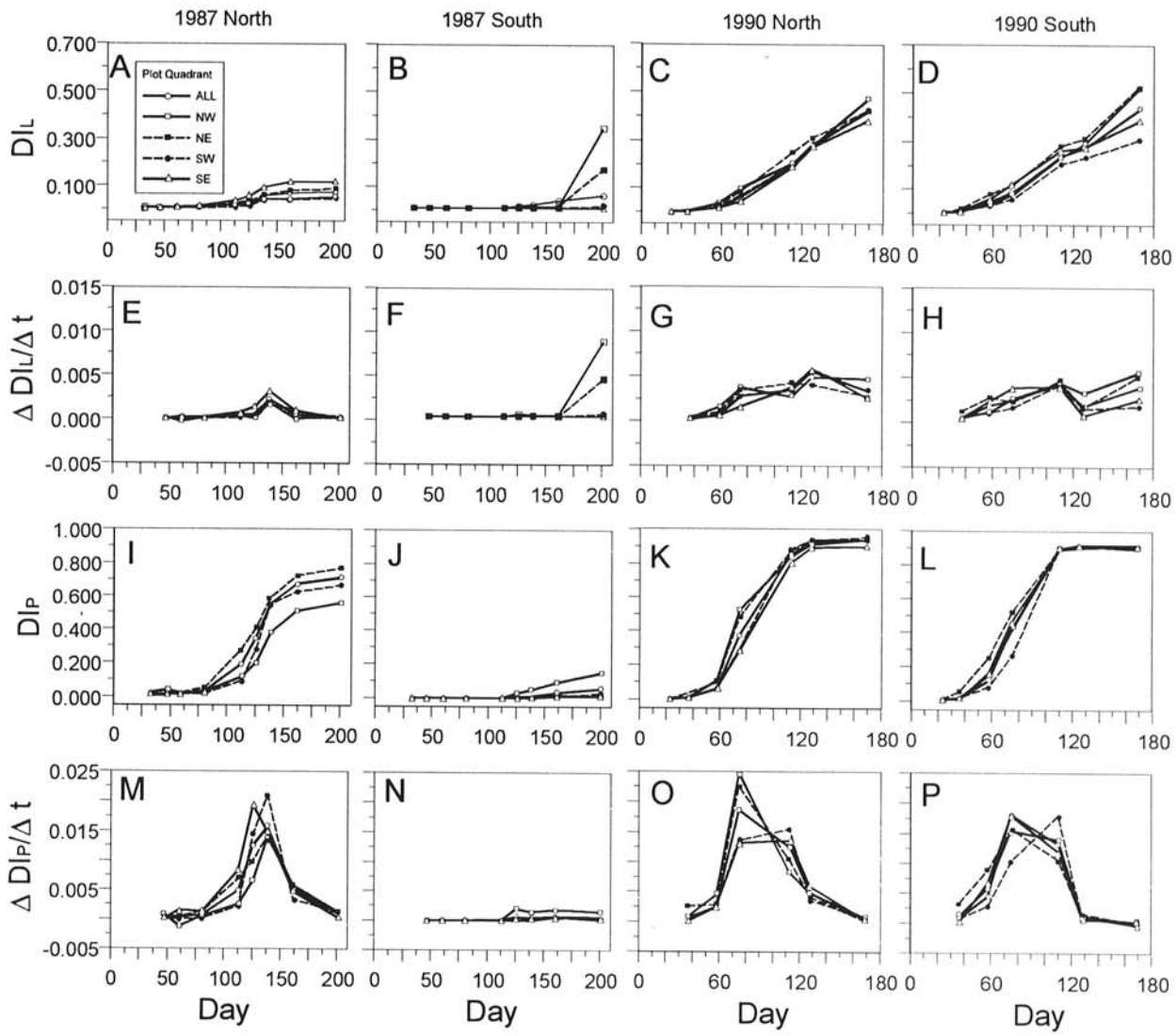

Fig. 1. Disease dynamics of citrus scab in four sour orange nursery plots. **A–D,** Disease incidence as DI_l = number of infected leaves per total number of leaves per plant, and **I–L,** disease incidence as DI_p = proportion of diseased plants. The change in the rate of disease incidence for **E–H,** $\Delta DI_l/\Delta T$ and **I–L,** $\Delta DI_p/\Delta T$, over time (t) in days, indicating the inflection point of the disease progress curve.

Each of the four plots was treated at approximately 30-day intervals for the duration of the experiment with one of the following fungicides: benomyl (Benlate 50WP, 0.30 g/liter), captafol (Difolatan 4F, 2.50 ml/liter), copper (Kocide 101, 0.96 g/liter), and water control to cause epidemics of differing severity.

TABLE 1. Regression analysis via the nonlinear Gompertz model of disease incidence of citrus scab in sour orange nurseries and chemical control plots over time

Plot[a]	Parameter[b]	Estimate	Asymptotic SE	Correlation observed vs. predicted[c]	Residual pattern[d]
Nursery: Trees (DI_p)					
87N	k_p	0.0221	0.0035	0.9800	–
	B	16.8572	7.8976		
87S	k_p	0.0062	0.0006	0.9850	–
	B	10.0291	1.1096		
90N	k_p	0.0505	0.0041	0.9988	–
	B	45.1083	14.3022		
90S	k_p	0.0495	0.0056	0.9972	–
	B	34.9917	14.6968		
Nursery: Leaves (DI_l)					
87N	k_l	0.0045	0.0008	0.9366	–
	B	6.1112	0.8232		
87S	k_l	0.0034	0.0003	0.9894	–
	B	10.6440	0.5492		
90N	k_l	0.0124	0.0009	0.9947	–
	B	6.7690	0.8206		
90S	k_l	0.0115	0.0008	0.9943	–
	B	5.6064	0.5839		
1988 chemical control: Trees (DI_p)					
Benomyl	k_p	0.0533	0.0041	0.9979	+
	B	131.0922	53.9722		
Water	k_p	0.0669	0.0046	0.9988	–
	B	321.3690	132.9594		
Copper	k_p	0.0459	0.0053	0.9951	–
	B	80.4555	45.7737		
Captafol	k_p	0.0199	0.0047	0.9444	–
	B	12.6109	8.0270		
1990 chemical control: Trees (DI_p)					
Benomyl	k_p	0.0713	0.0177	0.9978	–
	B	1,936.0928	3,850.3043		
Water	k_p	0.0964	0.0271	0.9975	–
	B	3,8924.0004	118,113.7064		
Copper	k_p	0.0305	0.0061	0.9856	–
	B	30.3695	22.4886		
Captafol	k_p	0.0064	0.0009	0.9719	–
	B	5.3631	0.6500		
1988 chemical control: Leaves (DI_l)					
Benomyl	k_l	0.0176	0.0021	0.9849	–
	B	10.4851	2.9467		
Water	k_l	0.0218	0.0020	0.9923	–
	B	15.3249	4.0846		
Copper	k_l	0.0113	0.0014	0.9771	–
	B	6.5472	1.3508		
Captafol	k_l	0.0067	0.0006	0.9848	–
	B	6.4919	0.6365		
1990 chemical control: Leaves (DI_l)					
Benomyl	k_l	0.0103	0.0008	0.9936	–
	B	7.0487	0.7702		
Water	k_l	0.0147	0.0010	0.9965	–
	B	12.5751	1.8119		
Copper	k_l	0.0108	0.0007	0.9962	–
	B	8.5696	0.9119		
Captafol	k_l	0.0032	0.0003	0.9775	–
	B	5.7183	0.2711		

[a] Plots: 87N = 1987 north; 87S = 1987 south; 90N = 1990 north; and 90S = 1990 south.

[b] Model parameters were estimated by nonlinear regression of the integrated Gompertz equations $y = 1 - \exp^{-Be^{-rt}}$, where r is the rate parameter (r_{ip} for disease incidence of plants and r_{il} for disease incidence of leaves), $B = -\ln(y_0)$, k is the rate parameter (k_p = the rate parameter for disease incidence of plants, and k_l = the rate parameter for disease incidence of leaves), y is disease measured as incidence of plants or leaves, and t is time in days.

[c] Coefficients of correlation (r^{*2}) of predicted values against observed.

[d] Presence (+) or absence (–) of patterns in plots of residuals of regression versus predicted values, indicating appropriateness of model fit to data.

Assessment of disease. Disease assessments were made throughout the 1987 (nine assessments), 1988 (nine assessments), and 1990 (eight assessments) seasons on all plants in all plots. Incidence of diseased leaves ($[DI_l]$ = the visually estimated number of infected leaves per total number of leaves per plant for each plant) and incidence of diseased plants ($[DI_p]$ = calculated proportion of diseased plants) were recorded for each plot on each assessment date.

Temporal analyses. The nonlinear forms of the exponential, monomolecular, logistic, and Gompertz models (7,25) were examined for their description of DI_l and DI_p over time for individual nursery and disease control plots by year. The appropriateness of each model was assessed by examination of residual plots and by correlation analysis of observed versus predicted values to determine the best model. For individual nursery plots, once the best model was selected (Gompertz) the data were reexamined by dividing the plot into four directional subplots whose common corner was the central focal plant to compare rates of disease progress in four directions away from the focus of infection. Apparent rates of disease progress were estimated for each of the subplots using the nonlinear form of the Gompertz model. The Gompertz rates of disease progress (k) among these directional subplots, as well as the rates of disease progress between subplots and the entire plot, were compared by t tests in an attempt to detect a predominant direction of disease increase.

Spatial analyses. The strength and directionality or orientation of aggregation of diseased plants in the four nursery plots was examined with spatial autocorrelation analysis using the LCOR2 software program because of its ability to handle quantitative values for each tree (13). For the spatial autocorrelation analysis, the [x,y] spatial location and DI_l values for each plant on each assessment date in the individual plots were used as input data. The program calculated proximity patterns of positively correlated lag positions (SL+). The size and shape of core and reflected clusters of SL+, strength of aggregation, angle of skewness of the proximity pattern away from the direction of the rows, as well as within-row, across-row, and edge effects were calculated.

Calculation of isopaths of similar disease incidence. Isopaths, at 0.1 disease-incidence increments, were generated from quadratized DI_l data via a geotopographical computer program (Surfer for Windows, Golden Software, Inc., Golden, CO) for each disease assessment date. This procedure allowed visualization of the location and extent of both the primary and secondary foci. Output data files generated by the geotopographical program were translated and imported into a computer automated design program (AutoCAD for Windows, version 11, Autodesk, Inc., Sausalito, CA) and corrected for scaling distortion. Distances from the focal plant to the boundary of each isopath contour line were measured by selecting appropriate points with the use of a digitizing tablet (SummaSketch Plus 1201, Summagraphics Corp., Fairfield, CT) and querying with the AutoCAD 'distance' subroutine. Distances were measured in eight compass directions (N, NE, E, SE, S, SW, W, and NW).

Disease gradients were calculated for each entire nursery plot and each of the four directional subplots by assessment date via disease gradient software for the PC (GRADCALC, version 2.2b, USDA/ARS, Orlando, FL) using 0.5-m concentric annuli around the central focal tree (11). Gradient data then were fitted to a gradient model of Gompertz-transformed disease incidence versus ln(distance) to determine the gradient slope (b). Parameter estimates obtained from the disease gradient and temporal analyses were used to calculate isopath velocity (v) by $v = ks|b^{-1}|$, for a given distance (s), where k is the Gompertz rate parameter. Rates of disease spread (v_s) were calculated for all plots at various distances (where s = 1, 5, 10, or 15 m) omnidirectionally from point inoculum sources for the nursery plots via GRADCALC and directionally from line sources of inoculum for disease control treatment plots to examine the effect of control strategies on pathogen spread.

Areas within individual isopath levels were integrated via a contour-volume subroutine of the geotopographical mapping program using a medium-weight kriging option to smooth the contours slightly and presented graphically for comparison. Three-dimensional response surfaces were prepared to visualize the dynamics of the areas within individual 0.1 increment isopath levels over time. Data from these response surfaces of isopath-bounded area (A_i) versus isopath level (I_α) and time (t) in days were subjected to nonlinear regression analyses within which 37,233 possible equations with up to 36,582 iterations of those models were compared (TableCurve3D for Windows, version 1.04, Jandel Scientific, San Rafael, CA). The goal was to select a common model that accounted for the most variation among all of the nursery isopath-surface-response data sets for a given year. The appropriateness of each model was determined by examining correlation coefficient (r^{*2}) of observed versus predicted values via SAS (SAS Institute, Inc., Cary, NC). Comparisons were made among the three-dimensional response surfaces via comparison of the Kolmogorov-Smirnov asymptotic test statistic (KSA) for each treatment based on the empirical distribution (step) function. A nonparametric analysis of variance of ranks was performed and the probability of a greater KSA (measure of the discrepancy between response surfaces) was calculated (8). These analyses provided a means of comparing spatio-temporal epidemic data to determine differences among disease control strategies.

RESULTS

For the 1987 nursery plots, progress of citrus scab followed asymmetrically sigmoid curves (Fig. 1A, B, C, D, I, and L) with inflection points occurring approximately 140 days after inoculum was introduced into the plots for DI_l and ranged from 125 to 140 days for DI_p for different directional gradients (Fig. 1E, F, M, and N). For the 1990 nursery plots, progress curves were associated with inflection points that ranged from 110 to 113 and 75 to 115 days for DI_l and DI_p, respectively (Fig. 1G, H, O, and P). The rapid increase in disease noted in the plots did not appear to be associated with any individual meteorological event but rather reflected the rapid buildup of disease in response to numerous rain showers and frequent overhead irrigation. Of the nonlinear models evaluated, the Gompertz model was the most appropriate for describing disease progress based on correlation of observed versus predicted values and examination of residual plots. Because of the large number of models tested and the large number of test plots, only the results of the Gompertz model fits are presented (Table 1).

The Gompertz rates of disease increase (k_l and k_p) for disease incidence of leaves (DI_l) and plants (DI_p), respectively, for the 1987 and 1990 nurseries were calculated and compared via paired t test (Table 2). Disease progression also was examined for each nursery divided into directional quadrants whose common corner

TABLE 2. Paired t test comparison of nonlinear Gompertz rate parameters (k) for disease incidence of citrus scab of trees (DI_P) or leaves (DI_l), temporal increase among directional quadrants in sour orange nursery plots

Plot[a]	Quadrant[b]	k	Asymptotic SE	df	t value[c]		
					NE	NW	SE
Disease incidence of plants (DI_P)							
87N	NE	0.0237	0.0027	14			
	NW	0.0153	0.0024	14	2.347*		
	SE	0.0448	0.0063	14	3.055**	4.367**	
	SW	0.0220	0.0048	14	0.301	1.264	2.854*
87S	NE	0.0050	0.0008	14			
	NW	0.0082	0.0008	14	2.929*		
	SE	0.0054	0.0014	14	0.262	1.784	
	SW	0.0080	0.0005	14	3.308**	0.229	1.797
90N	NE	0.0535	0.0066	10			
	NW	0.0481	0.0075	10	0.541		
	SE	0.0441	0.0040	10	1.217	0.465	
	SW	0.0561	0.0036	10	0.347	0.960	2.227
90S	NE	0.0412	0.0040	10			
	NW	0.0504	0.0072	10	1.110		
	SE	0.0470	0.0058	10	0.816	0.372	
	SW	0.0579	0.0087	10	1.733	0.662	1.044
Disease incidence of leaves (DI_l)							
87N	NE	0.0046	0.0007	14			
	NW	0.0033	0.0006	14	1.489		
	SE	0.0051	0.0009	14	0.465	1.676	
	SW	0.0034	0.0007	14	1.189	0.128	1.439
87S	NE	0.0342	0.0008	14			
	NW	0.0379	0.0016	14	1.733		
	SE	0.0036	0.0007	14	30.143**	19.297**	
	SW	0.0153	0.0001	14	24.761**	13.723**	17.035**
90N	NE	0.0117	0.0012	10			
	NW	0.0128	0.0005	10	0.902		
	SE	0.0117	0.0013	10	0.032	0.793	
	SW	0.0123	0.0008	10	0.451	0.505	0.387
90S	NE	0.0127	0.0007	10			
	NW	0.0144	0.0005	10	1.963		
	SE	0.0096	0.0012	10	2.197	3.668**	
	SW	0.0090	0.0013	10	2.450*	3.824**	0.326

[a] Plots: 87N = 1987 north; 87S = 1987 south; 90N = 1990 north; and 90S = 1990 south. DI_P = proportion of diseased plants; DI_l = number of diseased leaves per total number of leaves per plant.

[b] NE = northeast, NW = northwest, SE = southeast, and SW = southwest.

[c] * = significantly different if greater than 2.228 at $P = 0.05$ with 10 df or greater than 2.145 with 14 df, and ** = significant if greater than 3.169 at $P = 0.01$ with 10 df or greater than 2.977 with 14 df, respectively. H_o: $k_1 = k_2$ and H_a: $k_1 \neq k_2$, where k_n = the slope value of the Gompertz model; df was 16 for all slope comparisons.

was the central focal plant. Anisotropy existed among directional quadrants for the k_p associated with DI_p for both 1987 plots and for k_l associated with DI_l for the 1987 south (87S) and 1990 south (90S) plots (Table 2). However, the directionality of spread was not consistent between the two plots planted at the same location each year.

TABLE 3. Spatial autocorrelation analysis and statistics for citrus scab in sour orange nurseries

Plot[a]	Date	Disease incidence[b]	Significant lags[c]		Strength of aggregation[d]	Core cluster size[e]	Reflected cluster size[f]	Total no. of clusters[g]	Angle of skewness[h]	Effects[i]		
			SL+	SL–						Within row	Across row	Edge
87N	29 Jun.	0.008	4	0	1.00	4	–	1	0	1	1	ns
	13 Jul.	0.012	6	0	1.00	6	–	1	0	4	1	ns
	28 Jul.	0.018	5	0	1.00	5	–	1	–29.5	2	0	ns
	17 Aug.	0.032	13	0	1.00	13	–	1	–28.3	3	2	ns
	18 Sep.	0.187	43	0	0.74	32	1,2,3	8	7.0	9	3	ns
	1 Oct.	0.351	67	66	0.79	53	1,2,3,6	6	9.9	11	5	ns
	14 Oct.	0.554	75	220	0.95	70	1,2,	4	13.5	15	5	ns
	6 Nov.	0.671	79	163	0.84	66	1,2,3,5	5	13.5	15	4	ns
	16 Dec.	0.708	71	108	0.83	59	1,2	7	15.2	13	4	ns
87S	1 Oct.	0.008	16	0	0.19	3	1,3,4	5	–22.1	2	1	ns
	14 Oct.	0.015	17	0	0.12	2	1,2,4	8	–19.3	2	0	ns
	6 Nov.	0.032	29	0	0.07	2	1,2,6	18	–17.7	2	0	ns
	16 Dec.	0.054	17	0	0	0	1,2	17	–18.8	0	0	ns
90N	31 Aug.	0.062	13	0	0.62	8	1,2	5	13.7	5	1	ns
	17 Sep.	0.380	16	1	0.56	9	1,2	5	19.0	8	1	ns
	15 Oct.	0.854	23	31	0.65	15	1,2,3	6	18.8	9	1	ns
	30 Oct.	0.923	25	25	0.52	13	4,7	3	–20.0	8	1	ns
	10 Dec.	0.931	13	2	0.54	7	1,3	4	20.7	6	1	ns
90S	9 Aug.	0.017	3	0	0	0	1	3	47.4	0	0	ns
	31 Aug.	0.146	13	0	0.031	4	1,2,4	6	19.0	2	1	ns
	17 Sep.	0.400	18	2	0.44	8	1,2,3	6	18.4	3	1	ns
	12 Oct.	0.868	13	4	0.69	9	1	5	21.5	3	2	ns
	30 Oct.	0.901	17	2	0.71	12	1	6	13.9	3	4	ns
	10 Dec.	0.896	51	2	0.43	22	1,2,24	4	6.9	7	3	ns

[a] Plots: 87N = 1987 north; 87S = 1987 south; 90N = 1990 north; and 90S = 1990 south.
[b] Number of scab-infected trees per total number of trees in the nursery; 1987 and 1990 nurseries had 1,007 and 403 each, respectively. Dates for which disease incidence was <0.001 are not shown.
[c] Number of [x,y] lags significantly greater (SL+) or less (SL–) than expected by chance at $\alpha = 0.05$.
[d] Number of SL+ in core cluster per total number of SL+.
[e] Number of significant SL+ lags contiguous with the [0,0] lag position that form a discrete group.
[f] Number of contiguous SL+ in various clusters not contiguous with the core cluster. – = not tested due to too few diseased trees in plot for comparison.
[g] Number of contiguous clusters of SL+ in the proximity pattern.
[h] The angle between two lines: the first line perpendicular with the row orientation and the second line defined by a line between the [0,0] lag position and the geographic centroid of SL+ values of diseased trees in plot. A positive value indicates that the orientation of the proximity pattern is rotated in a clockwise direction from the row orientation, whereas a negative value indicates a counterclockwise rotation. The greater the angle the more intense the skewness of the pattern.
[i] Row and column effects = the number of SL+ within-row and within-column of the row and column defined by the [0,0] lag. Edge effects are significant (S) or nonsignifcant (ns) if the number of SL+ at the distal edges of the proximity pattern per the total number of SL+ is ≥5% and <5%, respectively.

TABLE 4. Paired *t* test comparison of nonlinear Gompertz rate parameters (*k*) of citrus scab temporal increase among disease control treatments in sour orange disease control plots

Year	Treatment	Rate (k_l)	Asymptotic SE	df	*t* value[a]		
					Water	Copper	Benomyl
Disease incidence of leaves (DI_l)[b]							
1988	Water	0.022	0.002				
1988	Copper	0.011	0.001	12	4.245**		
1988	Benomyl	0.018	0.002	12	1.462	2.499*	
1988	Captafol	0.007	0.001	12	7.215**	2.986*	5.095**
1990	Water	0.015	0.001				
1990	Copper	0.011	0.001	10	3.287**		
1990	Benomyl	0.010	0.001	10	3.604**	0.466	
1990	Captafol	0.003	0.000	10	11.308**	9.649**	8.557**
Disease incidence of trees (DI_p)[b]							
1988	Water	0.067	0.005				
1988	Copper	0.046	0.005	12	2.993*		
1988	Benomyl	0.053	0.004	12	2.198*	1.115	
1988	Captafol	0.020	0.005	12	7.116**	3.666**	5.352**
1990	Water	0.096	0.027				
1990	Copper	0.030	0.006	10	2.371*		
1990	Benomyl	0.071	0.018	10	0.777	2.182	
1990	Captafol	0.006	0.001	10	3.315**	3.895**	3.665**

[a] * and ** = significantly different at $\alpha = 0.05$ (if $t > 2.228$ with 10 df or $t > 2.179$ with 12 df, respectively) and $\alpha = 0.01$, respectively. Treatments were applied on approximately 30-day intervals by tank-sprayer application.
[b] DI_p = proportion of diseased plants; DI_l = number of diseased leaves per total number of leaves per plant.

Aggregation of disease was demonstrated with spatial autocorrelation analysis by the presence of clusters of significantly positive lag (SL+) positions (Table 3). Greater aggregation of scab-diseased plants occurred within rows compared to across rows for all four nursery plots, with the exception of the 1990 south plot (90S) on 30 October (Table 3). For three of the four nursery plots, the strength of aggregation was moderate to high due to the presence of a single scab-diseased focal tree and conservation of the resulting aggregated pattern. For the 1987 south plot (87S), in which no central focal tree was used, the strength of aggregation was lower and did not occur until midseason, concurrently with the first appearance of disease from exogenous sources. Reflected clusters of SL+ positions were common for all four nursery plots and consisted of 1 to 24 SL+, corresponding to the formation of secondary foci of infection. No significant edge effects were noted for any of the plots or assessment dates.

The Gompertz rates for temporal increase were compared among the 1988 and 1990 disease control test plots by paired t test (Table 4). As expected, captafol lowered k_p and k_l more than any other treatment. For the disease incidence of trees, there was no significant difference between k_p for copper treatment for 1988 or 1990 versus the benomyl treatment corresponding to each of the years, and there was no significant difference between the k_l for 1988 and k_p for 1990 for benomyl compared to the water control.

The dynamics of v (rate of disease spread) for the two 1990 uncontrolled nursery plots (90S and 90N) were different. Although nursery plots were treated identically and were established at the same location, the rate of spread accelerated a few days earlier in the north plot (90N), then leveled off, whereas spread began a few days later and continued to increase in the south plot (90S) until the end of the season (Fig. 2A). For the 1988 disease control strategy plots, the rate of spread of scab was highest initially then diminished over the rest of the season in the water control and benomyl-treated plots, whereas the rate remained low throughout the season for the captafol plot (Fig. 2B). For the 1990 disease control plots, the rate of spread decreased with a resurgence of disease increase in midseason for the water control plot, whereas the three chemical control plots all resulted in a continual reduction in disease spread throughout the season (Fig. 2C).

Because of the development of numerous secondary foci resulting from splash dispersal, the disease gradient models often fit the data poorly (data not shown) (13). Therefore, as an alternative, isopath-bounded areas were calculated directly via area integration from disease contour maps (Figs. 3, 4, and 5), and the change in individual isopath areas over time ($\Delta A_i/\Delta t$) were examined for each plot. Results from nonlinear regression analyses for response surfaces of isopath-bounded area in square meters (A_i) versus isopath level (I_α) and time (t) in days are shown in Table 5. The nonlinear model that accounted for the most variation among all of the nursery isopath-surface-response data sets for a given year was the log-normal additive with synergy and intercept (LNASI):

$$A_i = a + b\exp\left\{-0.5\left[\frac{\ln\left(\frac{I_\alpha}{c}\right)}{d}\right]^2\right\} + e\exp\left\{-0.5\left[\frac{\ln\left(\frac{t}{f}\right)}{g}\right]^2\right\} + h\exp\left\{-0.5\left[\frac{\ln\left(\frac{I_\alpha}{c}\right)}{d}\right]^2 + -0.5\left[\frac{\ln\left(\frac{t}{f}\right)}{g}\right]^2\right\}$$

where a, b, c, d, e, f, and g are constants. The general model fit all of the data sets well ($r^{*2} \geq 0.97$) (Table 5). Each resulting three-dimensional response surface represents the spatio-temporal isopath dynamics for individual plots over the duration of the epidemic (Figs. 6 and 7). The modeled shapes of the response surfaces are all similar. For the three uncontrolled scab nursery plots with central foci of infection (87N, 90S, and 90N), the response surface representing the 1987 plot (Fig. 3) was less extensive compared to either of the 1990 plots (Figs. 4 and 5) because disease was slower to develop and higher disease incidence values were uncommon, resulting in the representation of lower isopath levels (0.1 to 0.4) exclusively (Fig. 6). Response surfaces representing the individual disease control strategy plots for 1988 and 1990 demonstrated differences in response surface shapes associated with each treatment (Fig. 7). The most and least extensive response surfaces were associated with the water control (least effective) and captafol (most effective) disease control plots, respectively.

Comparisons among all the spatio-temporal data sets indicated that captafol significantly ($P < 0.05$) reduced, spatio-temporally, the associated epidemic compared to all other control strategies for both years, whereas none of the other control strategies differed spatio-temporally (Table 6). The significance between the spatio-temporal data sets was marginal ($P = 0.054$) for some of the comparisons (i.e., observed data sets), whereas the differences became more pronounced ($P = 0.0001$) when the model was used to generate predicted values that were then compared (Table 6).

DISCUSSION

For the 1987 (87N) and 1990 (90S and 90N) nursery plots with a point focus of infection, disease progress for DI_l and DI_p was well described by the nonlinear Gompertz model. Differences in

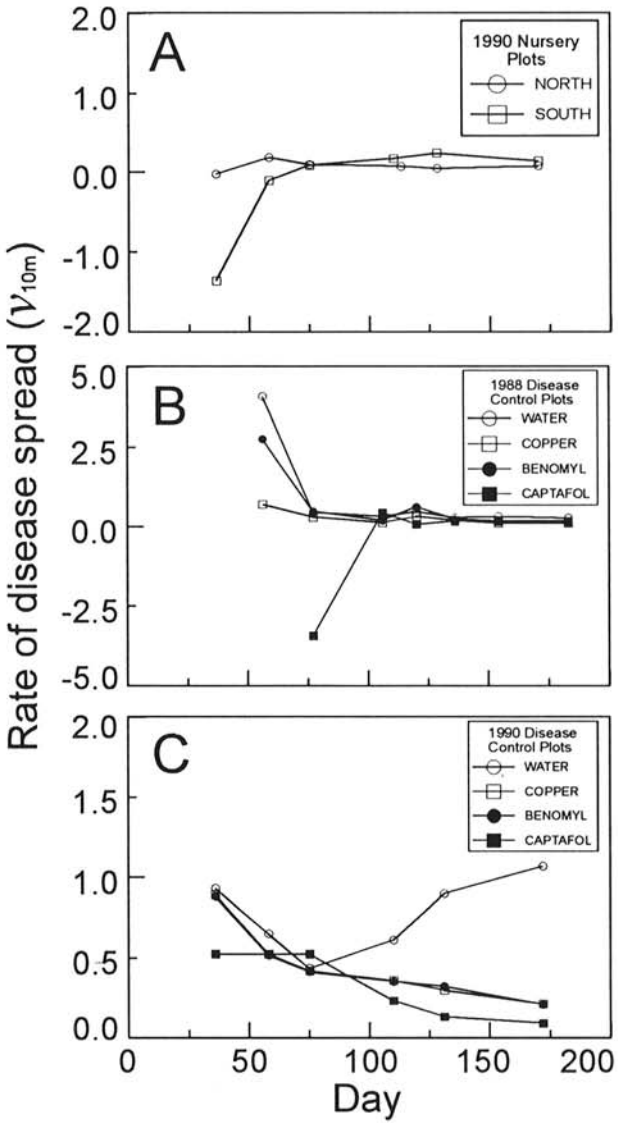

Fig. 2. Rates of disease spread over time emanating from point foci of infection of citrus scab in experimental sour orange nurseries. Rates (v) = the rate of disease spread, $v = rs|b^{-1}|$, where s indicates the distance from the focus of infection based on the integrated model $-\ln[-\ln(y)] = a^* - b\ln(s) + kt$, where y = disease incidence, b = the slope of disease incidence over distance s, t = time in days, and k = the Gompertz rate of disease increase. Rates presented were calculated for a 10-m distance from the focus of infection, i.e., v_{10m}.

temporal progress among directional quadrants of citrus nurseries during the same year and at the same location were inconsistent. The lack of a common preferential direction suggests that temporal increase probably was associated more with the effect of splash dispersal due to overhead irrigation and rain than prevailing winds. This indicates that the predominant inoculum was probably the ellipsoid hyaline conidia, which are thought to be splash-dispersed (32,35), and not the spindle-shaped, pigmented conidia, which are thought to be disseminated more favorably by wind (32,35). Disease progress in the disease control plots for both years also was best described by the Gompertz model with the exception of data for DI_p for the benomyl and water control plots for 1990, which were fit well by the Gompertz model, but had relatively high error terms. All disease control treatments with the exception of benomyl significantly affected the rate of disease increase for both DI_p and DI_l.

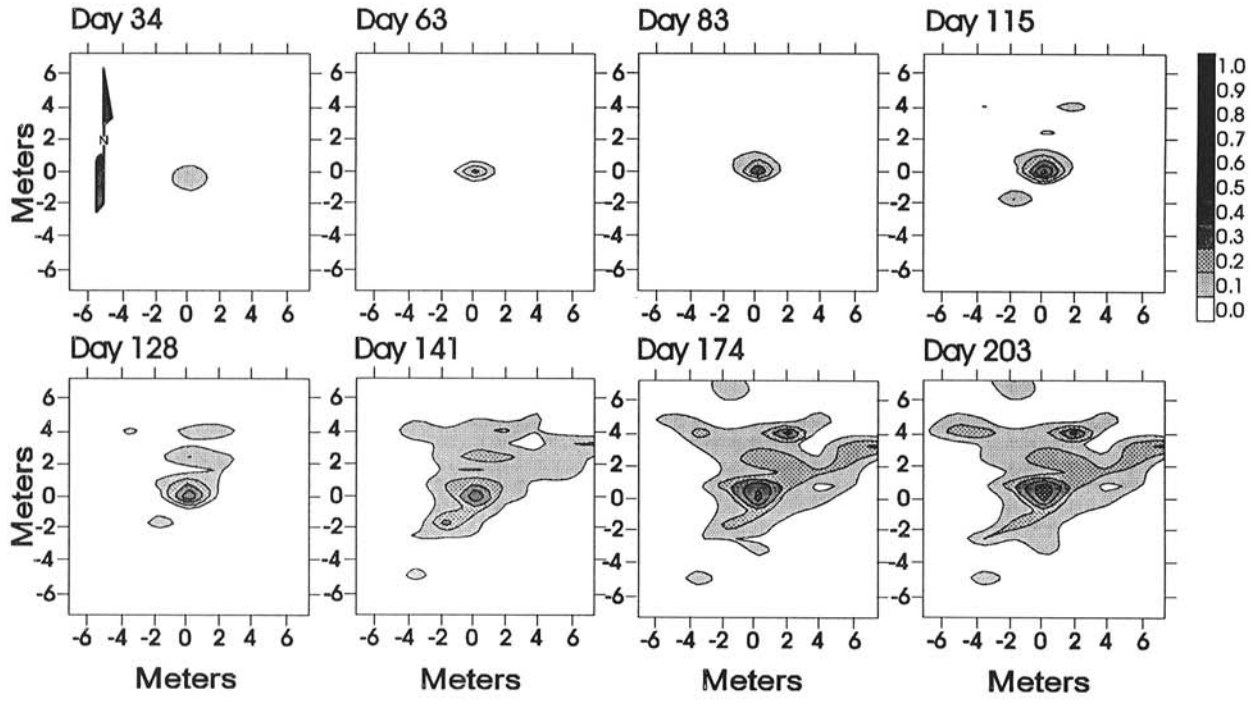

Fig. 3. Isopath contour maps of citrus scab in the 1987 north (87N) sour orange nursery plot for the assessment days indicated. Increasing isopath levels of disease incidence are represented by increasing gray scale and are indicated on the sidebar. There was a predominately northeastern movement of citrus scab isopaths away from the central point focus on days 128 through 207.

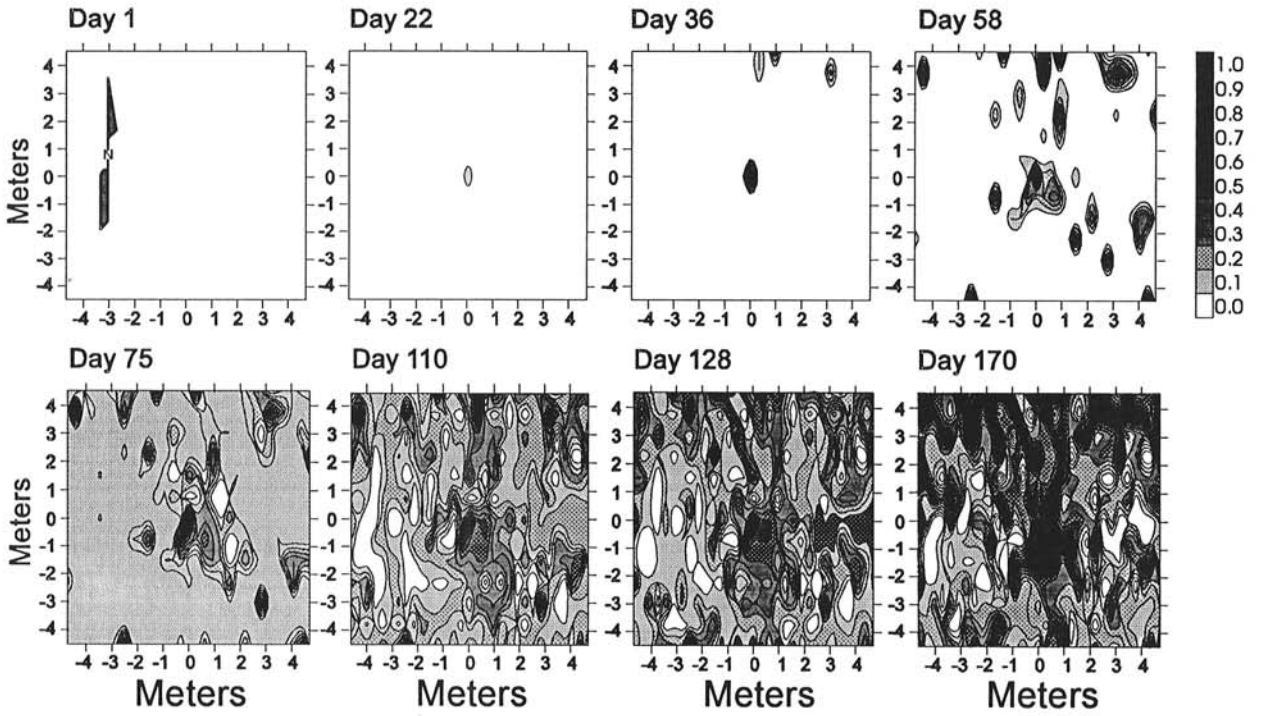

Fig. 4. Isopath contour maps of citrus scab in the 1990 south (90S) sour orange nursery plot for the assessment days indicated. Increasing isopath levels of disease incidence are represented by increasing gray scale and are indicated on the sidebar. There was predominately northeastern movement of citrus scab isopaths away from the central point focus on days 58 through 75.

The dynamics of isopath velocity, v, of citrus scab were very useful in describing differences among both untreated nurseries and disease control test plots. For the two identically maintained nursery plots at the same location in 1990, the dynamics of v were divergent with an acceleration in spread occurring earlier in one plot. For the chemical control plots in both 1988 and 1990, v diminished continually over the season with the exception of the 1990 water control plot. As anticipated, this decrease in the isopath velocity was more pronounced for the captafol-treated plots and less pronounced for the water control treated plots. All chemical control treatments except benomyl restricted disease spread, presumably due to reduced infection resulting from protection of tissues and leading to reduced production of secondary inoculum.

Secondary foci of disease developed and spread due to splash-dispersal of inoculum, although dry-dispersal of pigmented conidia is possible but less likely (31). The greater strength of disease aggregation in two of the nursery plots during the early part of the epidemic was directly related to the stability of the primary focus and the establishment of secondary foci emanating from it. As disease incidence exceeded 50% of the plants in the nursery, primary and secondary foci began to coalesce. Aggregation occurred both within and across rows but was stronger within rows. Dispersal of inoculum was more efficient for the closer plant spacing within rows compared to across rows. This often gave rise to oblong proximity patterns of aggregation. Lack of edge effects provided evidence that the majority of scab inoculum originated from within-plot sources rather than from external sources. Therefore, the plant-to-plant distance within the close, regular lattice spacing of plants in the simulated nurseries was considerably less than was necessary for dispersal to be effective. This was demonstrated further by the development of secondary foci often several rows distant from the primary focus of disease. It also was noted that the orientation of the long axis of the spatial autocorrelation proximity patterns was skewed compared to the orientation of the rows. This angle of skewness changed over time in response to dispersal, giving rise to new infections, and indicated that the spatial processes affecting the orientation of dispersal of inoculum were neither orientated along the rows nor consistent in orientation over time.

The occurrence of numerous secondary foci during the epidemic occasionally resulted in poor fits to the Gompertz disease gradient model on which disease-spread calculations were based and prompted the reliance on isopath dynamics as a means of estimating spatio-temporal disease increase (Figs. 3, 4, and 5). In the chemical disease control plots, movement of some isopath levels occasionally reversed direction during the epidemic and receded toward the focus. These reversals were associated with the growth of host tissues that did not become infected, resulting in a reduction in DI_t.

Rates of disease spread (v = isopathic velocity) decrease with increasing isopath levels (1), and individual isopath levels can be described as increasing (acceleration), decreasing (deceleration), or remaining constant (21). The dynamics of isopath rates, when related to biological and meteorological events such as host growth and weather, provided insight into disease dynamics. Isopath velocity fluctuated throughout the epidemics in this study. Thus, a general rate of isopath velocity or disease spread could not be determined for citrus scab. Acceleration of the movement of isopath

TABLE 5. Comparison of observed versus predicted values for nonlinear three-dimensional response surface models of isopath area (A_i) versus isopath level (I_α) and time in days (t) for citrus scab epidemics in experimental sour orange nurseries by treatment[a]

Treatment	Year	r^{*2}[b]	Year	r^{*2}
Water control	1988	0.972	1990	0.998
Copper	1988	0.985	1990	0.986
Benomyl	1988	0.979	1990	0.992
Captafol	1988	0.994	1990	0.990

[a] Response surface models were based on the log-normal additive with synergy and intercept equation shown in text.

[b] r^{*2} = coefficients of determination of correlation of predicted values against observed values.

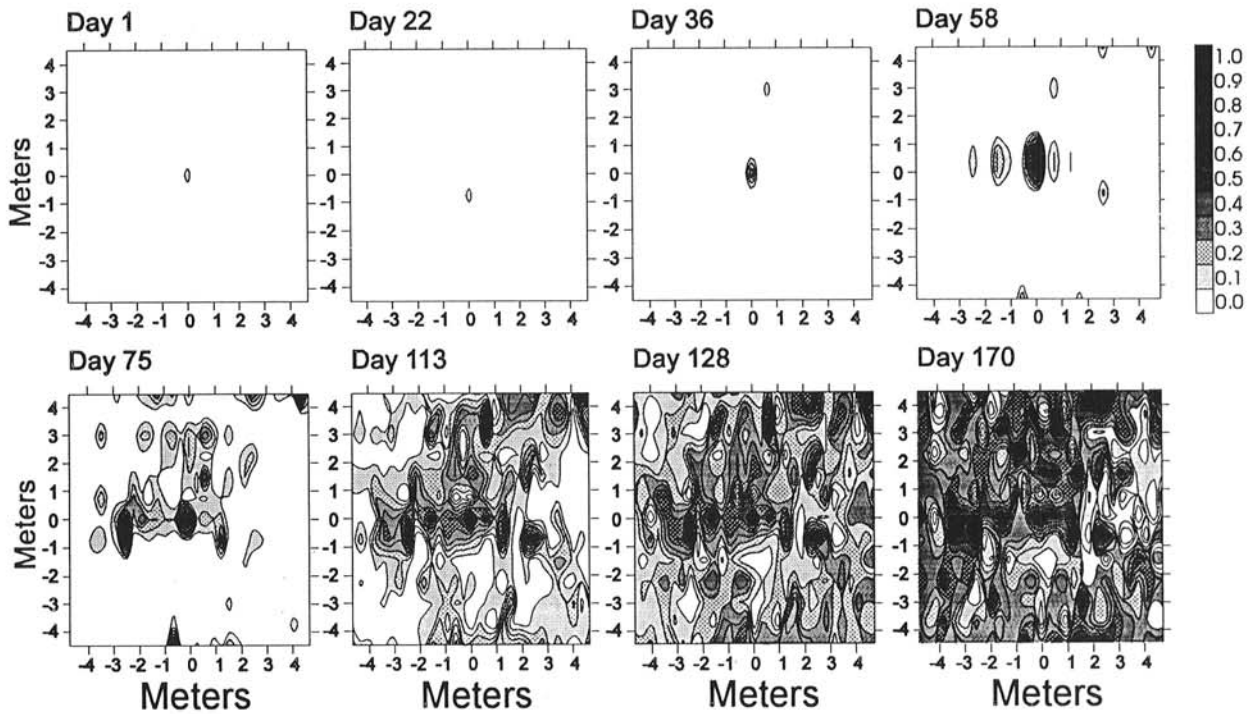

Fig. 5. Isopath contour maps of citrus scab in the 1990 north (90N) sour orange nursery plot for the assessment days indicated. Increasing isopath levels of disease incidence are represented by increasing gray scale and are indicated on the sidebar. There was predominately northern movement of citrus scab isopaths away from the central point focus on day 75.

boundaries (increased rate of spread) away from the focus was due to increasingly higher amounts of infection of new growth over time. Deceleration of isopath velocity (decreased rate of spread) was probably related to limited amounts of new infection. Reversal of direction of movement of some isopaths was described above.

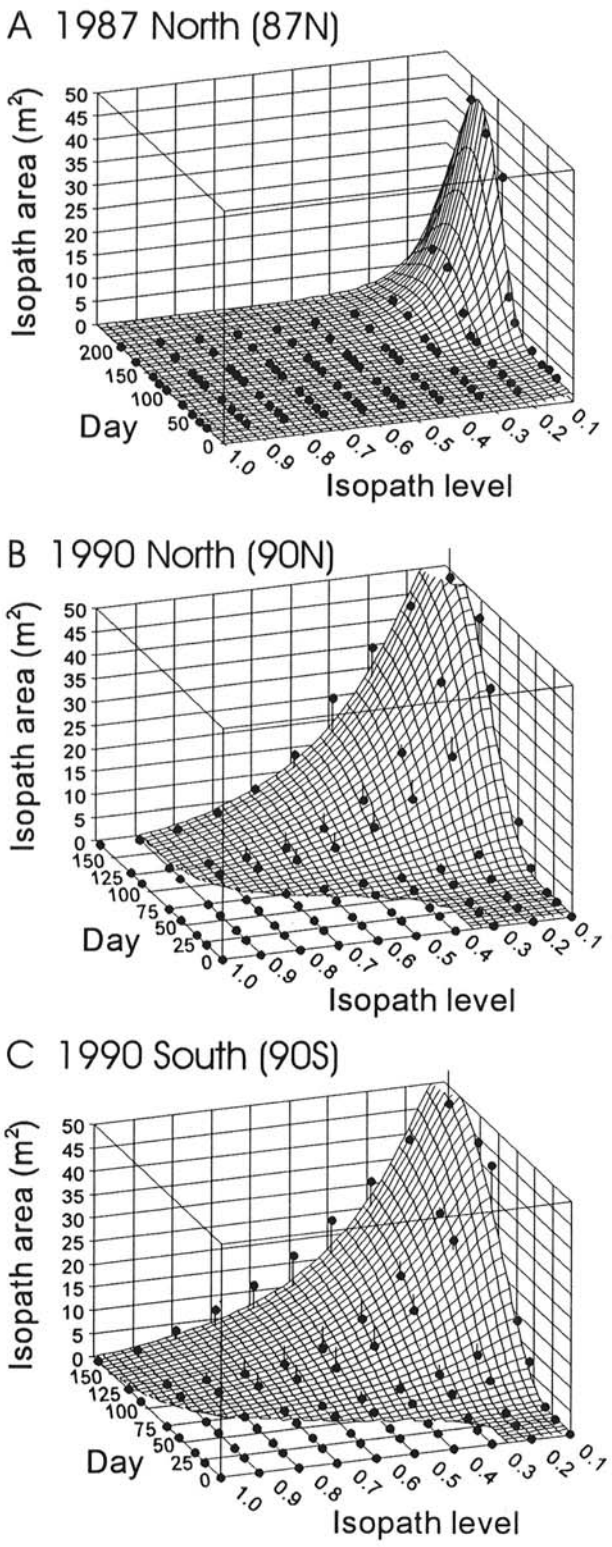

Fig. 6. Spatio-temporal response surface representations of citrus scab epidemics in sour orange **A,** in one nursery in 1987 and **B and C,** two nurseries in 1990. Black dots indicate observed data values. Wire-mesh response surfaces represent values predicted by the log-normal additive with synergy and intercept nonlinear model. Vertical lines extending from black dots to response surface demonstrate over or under prediction of model for each isopath level × isopath area.

On some occasions, lower isopath disease levels accelerated, whereas higher isopath levels decelerated during the same period of time. This seeming incongruity may be explained best by examining newly formed host tissue versus infection. Lower isopath levels expanded more rapidly due to low levels of infection on some new growth of some previously infected plants. Conversely, the accumulation of new host tissue with little or no new infections on previously and more severely diseased plants may have reduced the disease incidence on these plants, resulting in a slowing of isopath movement and, at times, a reversal of direction.

When citrus scab epidemics were examined graphically by plotting the isopath area (A_i) versus individual isopath levels (I_α) and time (t) in days, a set of three-dimensional response surfaces was visualized for which the shapes were strikingly similar but which varied in magnitude of isopath area (Figs. 6 and 7). This prompted the search for a common mathematical model that could adequately describe spatio-temporally the family of citrus scab epidemics studied. The LNASI model, described previously, accounted for >95% of the variation, and values predicted by the models had very high coefficients of correlation, ($r^{*2} > 0.97$) with the observed values. Using both the observed spatio-temporal data and the smoothed spatio-temporal data predicted by the models, the individual epidemics were compared with a nonparametric statistical test. This approach provided a valuable means of comparing individual epidemics and demonstrated that captafol was capable of reducing citrus scab incidence spatio-temporally, whereas other control strategies were not.

Captafol was a historically important control strategy for citrus scab, but the fungicide is no longer registered for use on citrus. Even so, the temporal, spatial, and spatio-temporal effects of captafol on citrus scab epidemics compared to the fungicides presently registered demonstrates the results of reducing inoculum production and infection.

In the disease control plots, captafol significantly reduced the rate of disease increase and the area bounded by individual isopath levels of disease. Occasional fluctuations in the isopath dynamics of the captafol plots were seen. For example, the increase in isopath area in the 1988 captafol plot, around day 120, was probably a result of inadequate suppression of sporulation and subsequent infection of new host tissue at that time due to spray scheduling. Subsequent new growth was adequately protected by reducing spore production from established lesions, resulting in a corresponding decrease in isopath area. Higher isopath levels developed only slightly in the captafol-treated plot and encompassed considerably less area in both captafol- and copper-treated plots compared to the water control plot. The areas bounded by lower level isopaths increased in the captafol plot during midseason and subsequently decreased. Captafol, to a greater extent, and copper, to a lesser extent, served to reduce the area bounded by isopaths of disease severity. In the case of captafol, the reduction tended to delay isopath movement, and, thus, the area circumscribed by all isopath severity levels (Figs. 6 and 7). The lack of significant disease control by benomyl likely is due to the presence of benomyl-resistant strains of *E. fawcettii* reported previously in Florida (37). Although copper application did not greatly decrease the area circumscribed by lower isopath levels, it did reduce or delay the development of areas of high disease incidence within the plot. The sour orange seedlings grew vigorously, and susceptible new growth was almost continuously present in all plots.

Because all treatments were applied on an approximately 30-day schedule, it is unlikely that susceptible new growth was completely protected at all times. The temporary increase in isopath-bounded areas in the captafol-treated plot demonstrates this. More frequent application of captafol likely would have reduced scab disease development further by more thoroughly protecting new growth and, in the case of captafol, by reducing pathogen sporulation (35). The benefit would have been questionable with benomyl or with copper, which has little antisporulating activity (35).

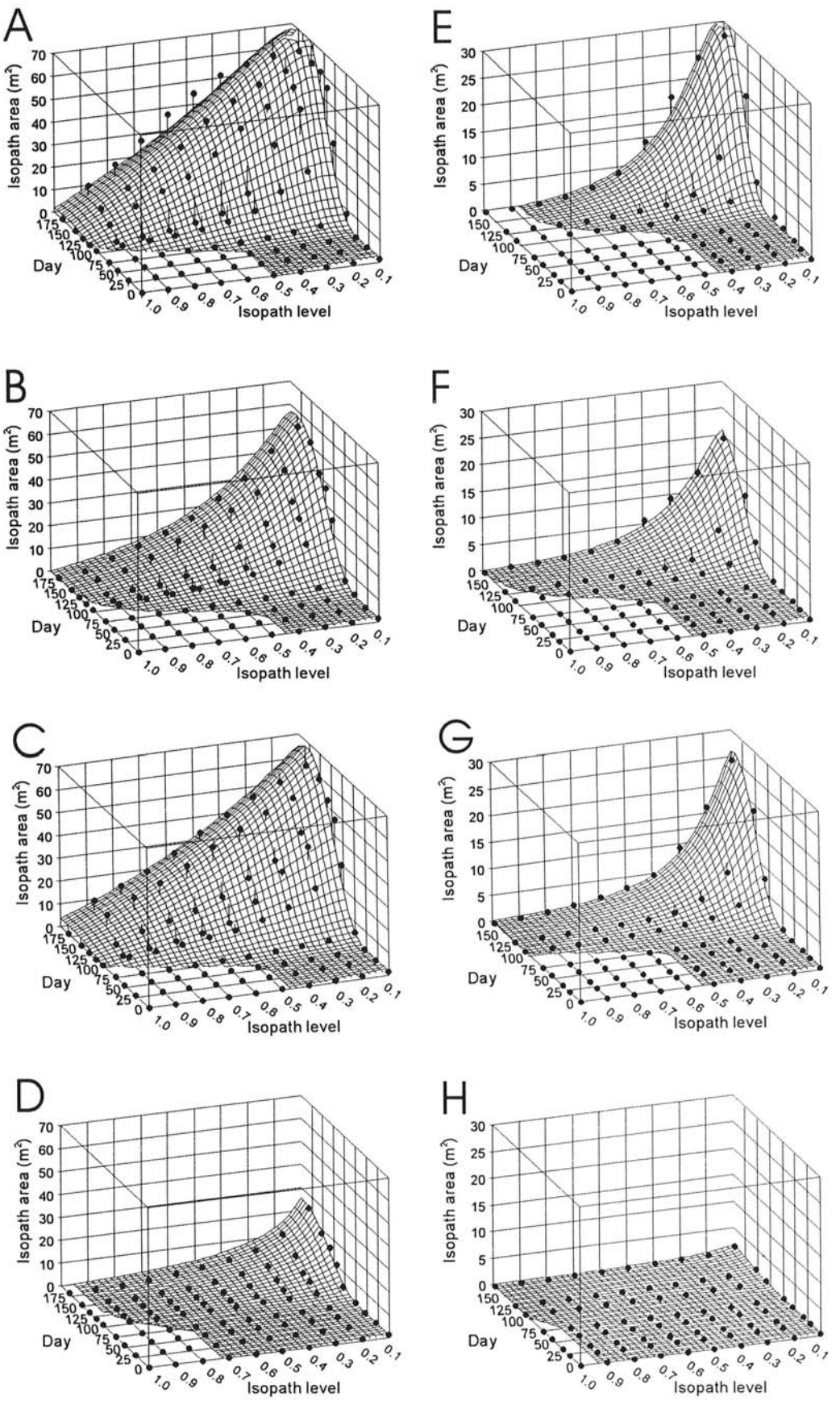

Fig. 7. Spatio-temporal response surface representations of citrus scab epidemics in sour orange under various control strategies **A–D,** during 1988 and **E–H,** during 1990. Control strategies compared were **A and E,** water control; **B and F,** copper; **C and G,** benomyl; and **D and H,** captafol. Black dots indicate observed data values. Wire-mesh response surfaces represent values predicted by the log-normal additive with synergy and intercept nonlinear model. Vertical lines extending from black dots to response surface demonstrate over or under prediction of model for each isopath level × isopath area.

TABLE 6. Nonparametric comparison of three-dimensional response surface data and models of isopath area (A_i) versus isopath level (I_α) and time in days (t) for citrus scab epidemics in experimental sour orange nurseries among treatments

Treatment	Year	Observed[a]			Predicted[a]		
		Copper	Captafol	Water	Copper	Captafol	Water
Benomyl	1988	0.820[b] (0.512)	2.162 (0.0002)	0.596 (0.869)	0.969 (0.305)	2.534 (0.0001)	0.560 (0.869)
Copper	1988		1.565 (0.015)	0.969 (0.305)		1.789 (0.003)	1.193 (0.116)
Captafol	1988			2.087 (0.0003)			2.460 (0.0001)
Benomyl	1990	0.474 (0.978)	1.344 (0.054)	1.423 (0.035)	1.265 (0.082)	1.976 (0.001)	2.530 0.0001
Copper	1990		1.344 (0.054)	1.660 (0.008)		2.214 (0.0001)	2.530 (0.0001)
Captafol	1990			1.344 (0.054)			2.925 (0.0001)

[a] Observed values represent comparisons of the unmodeled data; predicted values represent comparisons of the data sets predicted by the associated log-normal additive with synergy and intercept models.

[b] Values indicate the nonparametric Kolmogorov-Smirnov asymptotic (KSA) test of two independent samples. The values in parentheses indicate the associated probability (P) of a greater KSA. The KSA is a measure of the discrepancy between the two response surfaces (i.e., distribution functions) being compared in the vertical direction. H_0: $F(x) = G(x)$, for all x from $-\infty$ to $+\infty$; H_1: $F(x) \neq G(x)$, for at least one value of x, where $F(x)$ and $G(x)$ represent the response surface functions being tested.

LITERATURE CITED

1. Agostini, J. P., Gottwald, T. R., and Timmer, L. W. 1993. Temporal and spatial dynamics of post bloom fruit drop of citrus in Florida. Phytopathology 83:485-490.
2. Alderman, S. C., Nutter, F. W., and Labrinos, J. L. 1989. Spatial and temporal analysis of spread of late leaf spot of peanut. Phytopathology 79: 837-849.
3. Berger, R. D. 1981. Comparison of the Gompertz and logistic equations to describe plant disease progress. Phytopathology 71:716-719.
4. Berger, R. D., and Luke, H. H. 1979. Spatial and temporal spread of oat crown rust. Phytopathology 69:1199-1201.
5. Bitancourt, A. A., and Jenkins, A. E. 1936. *Elsinoe fawcettii*, the perfect stage of the citrus scab fungus. Phytopathology 26:393-396.
6. Bitancourt, A. A., and Jenkins, A. E. 1937. Sweet orange fruit scab caused by *Elsinoe australis*. J. Agric. Res. 54:1-18.
7. Campbell, C. L., and Madden, L. V. 1990. Introduction to plant disease epidemiology. John Wiley and Sons, New York.
8. Conover, W. J. 1980. Practical nonparametric statistics. 2nd ed. John Wiley and Sons, New York.
9. Fawcett, H. S. 1921. Some relations of temperature to growth and infection in the citrus scab fungus, *Cladosporium citri*. J. Agric. Res. 21:243-254.
10. Fawcett, H. S. 1936. Citrus diseases and their control. McGraw-Hill, New York.
11. Gottwald, T. R., Miller, C., Brlansky, R. H., Gabriel, D. W., and Civerolo, E. L. 1989. Analysis of the spatial distribution of citrus bacterial spot in a Florida citrus nursery. Plant Dis. 73:297-303.
12. Gottwald, T. R., Reynolds, K. M., Campbell, C. L., and Timmer, L. W. 1992. Spatial and spatiotemporal autocorrelation analysis of citrus canker epidemics in citrus nurseries and groves in Argentina. Phytopathology 82:843-851.
13. Gottwald, T. R., Richie, S. M., and Campbell, C. L. 1992. LCOR2—Spatial autocorrelation analysis software for the personal computer. Plant Dis. 76:213-215.
14. Gregory, P. H. 1968. Interpreting plant disease dispersal gradients. Annu. Rev. Phytopathol. 6:189-212.
15. Hearn, C. J., and Childs, J. F. L. 1969. A systemic fungicide effective against sour orange scab disease. Plant Dis. Rep. 53:203-205.
16. Hearn, C. J., Childs, J. F. L., and Fenton, R. 1971. Comparison of benomyl and copper sprays for control of sour orange scab of citrus. Plant Dis. Rep. 55:241-243.
17. Jeger, M. J. 1983. Analyzing epidemics in time and space. Plant Pathol. 32:5-11.
18. Jeger, M. J. 1984. Models of focus expansion in disease epidemics. Pages 269-288 in: The Movement and Dispersal of Agriculturally Important Biotic Agents: Int. Conf. Movement Dispersal Biotic Agents. Claitor, Baton Rouge, LA.
19. Jenkins, A. E. 1931. Development of citrus-scab organism, *Sphaeceloma fawcettii*. J. Agric. Res. 42:545-558.
20. Madden, L. V. 1980. Quantification of disease progression. Prot. Ecol. 2: 159-176.
21. Minogue, K. P., and Fry, W. E. 1983. Models for the spread of disease: Model description. Phytopathology 73:1168-1173.
22. Minogue, K. P., and Fry, W. E. 1983. Models for the spread of disease: Some experimental results. Phytopathology 73:1173-1176.
23. Modjeska, J. S., and Rawlings, J. O. 1983. Spatial correlation analysis of uniformity data. Biometrics 39:373-384.
24. Moherek, E. A. 1970. Disease control in Florida citrus with difolatan fungicide. Proc. Fla. State Hortic. Soc. 83:59-65.
25. Pennypacker, S. P., Knoble, H. D., Antle, C. E., and Madden, L. V. 1980. A flexible model for studying plant disease progression. Phytopathology 70:232-235.
26. Ruehle, G. D., and Thompson, W. L. 1939. Commercial control of citrus scab in Florida. Fla. Agric. Exp. Stn. Bull. 337.
27. Thal, W. M., Campbell, C. L., and Madden, L. V. 1984. Sensitivity of Weibull model parameter estimates to variation in simulated disease progression data. Phytopathology 74:1425-1430.
28. Van den Bosch, F., Frinking, H. D., Metz, J. A. J., and Zadoks, J. C. 1988. Focus expansion in plant disease. III: Two experimental examples. Phytopathology 78:919-925.
29. Van den Bosch, F., Zadoks, J. C., and Metz, J. A. J. 1988. Focus expansion in plant disease. I: The constant rate of focus expansion. Phytopathology 78:54-58.
30. Van der Plank, J. E. 1963. Plant diseases: Epidemics and control. Academic Press, New York.
31. Whiteside, J. O. 1974. Evaluation of fungicides for citrus scab control. Proc. Fla. State Hortic. Soc. 87:9-14.
32. Whiteside, J. O. 1975. Biological characteristics of *Elsinoe fawcettii* pertaining to the epidemiology of sour orange scab. Phytopathology 65:1170-1177.
33. Whiteside, J. O. 1978. Pathogenicity of two biotypes of *Elsinoe fawcettii* to sweet orange and some other cultivars. Phytopathology 68:1128-1131.
34. Whiteside, J. O. 1979. Citrus scab control with benomyl in relation to time of spraying and sites of fungicide deposition. Plant Dis. Rep. 63: 553-557.
35. Whiteside, J. O. 1980. Epidemiology and control of citrus scab in Florida. Pages 200-204 in: Proc. Int. Soc. Citriculture, Griffith, Aust. Florida Agricultural Experiment Station Journal Series 1270, University of Florida, Gainesville.
36. Whiteside, J. O. 1980. Detection of benomyl-tolerant strains of *Elsinoe fawcettii* in Florida citrus groves and nurseries. Plant Dis. 64:871-872.
37. Whiteside, J. O. 1981. Evolution of current methods for citrus scab control. Proc. Fla. State Hortic. Soc. 94:5-18.
38. Whiteside, J. O. 1988. Factors contributing to the rare occurrence of scab on sweet orange in Florida. Plant Dis. 72:626-628.
39. Winston, J. R. 1923. Citrus scab: Its cause and control. U.S. Dep. Agric. Bull. 1118.
40. Yamada, S. 1961. Epidemiological studies on the scab disease of Satsuma orange and its control. Tokai-Kini Natl. Agric. Exp. Stn. Spec. Bull. 2.